Earthline Journal of Chemical Sciences
E-ISSN: 2581-9003; CODEN: EJCSB4
Volume 13, Number 2, May 2026, Pages 139-154
https://doi.org/10.34198/ejcs.13226.11.139154

Effect of BN-bonds on tricyclo[6.2.0.02,5]deca-1(8),2(5),3,6,9-pentaene and tricyclo[6.2.0.03,6]deca-1(8),2,4,6,9-pentaene – DFT treatment

Lemi Türker

Department of Chemistry, Middle East Technical University, Üniversiteler, Eskişehir Yolu No: 1, 06800 Çankaya/Ankara, Turkey
e-mail: lturker@gmail.com; lturker@metu.edu.tr

Abstract

Perturbation effects of two BN-bonds on certain tricyclo pentaene structures having 10 ring atoms in their π-skeleton and two cyclobutene rings have been considered. Insertion of BN-bonds in the embedded cyclobutene moieties allows various regioisomers to arise. The structures have been investigated within the constraints of density functional theory at the level of B3LYP/6-311++G(d,p). The collected data have revealed that the optimized structures of them have exothermic heats of formation and favorable Gibbs free energy of formation values. They are thermally favored and electronically stable at the standard states. Various structural and quantum chemical data have been collected and discussed, including UV-VIS spectra.

1. Introduction

Annulenes are interesting monocyclic π-conjugated systems. However, there exist some structures, like corannulene, which have many rings but their peripheral skeleton resemble an annulene. In that respect structures shown in Figure-1 might be interesting systems themselves. In embedded form they might be present in some structures mentioned in the literature [1-4]. Moreover, their BN-bond(s) embedded perturbed forms would exhibit some quire behavior.

The tricyclo compounds having 10 carbons, namely tricyclo[6.2.0.02,5]deca-1(8),2(5),3,6,9-pentaene (A) and tricyclo[6.2.0.03,6]deca-1(8),2,4,6,9-pentaene (B) are both even alternant systems [5]. Figure 1 shows structures of them.

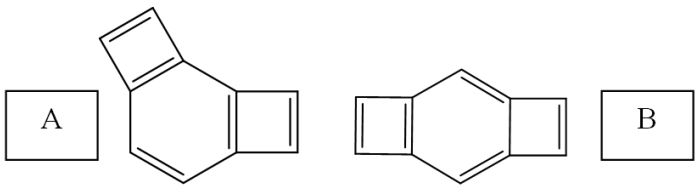

Figure 1. Structures of the parent molecules.

The literature reports that the B-N covalent-bond-embedded (trivalent B and N atoms) π-conjugated moieties are suitable to act as electron-rich units in order to construct electron-donor materials. Note that they have high-lying energy levels, good co-planar backbone, and high hole mobility. However, their absorption bands should be further broadened to lower energy (600–800 nm) in order to enhance the light harvesting ability [1].

The pioneering of BN-heteroarene research began in the late 1950s with Dewar's studies of polycyclic

Received: January 30, 2026; Accepted: March 4, 2026; Published online: March 8, 2026
Keywords and phrases: BN bonds, regioisomers, annulenes, spectra, DFT calculations.

derivatives of BN-naphthalenes, phenanthrene, and tetraphenes. The early syntheses of these compounds most often required harsh conditions and products obtained were in low overall yields [4]. The developments of photoisomerization [6] and Diels-Alder cycloaddition [7] of 1,2-azaborines to form heteroatom-substituted cyclobutane and cyclohexane derivatives, respectively, represented promising initial results toward this development. Recently, further achievements in azaborine chemistry have highly facilitated construction/ insertion of BN-bond(s) [8,9].

In some of the articles the structures having embedded tricyclo moieties mentioned above have been the points of interest [10-12]. Arisawa et al., studied dicyclobutabenzenes (linear) and (curved) [10] (which possess the same sigma-skeleton with the parent compounds presently mentioned). They constitute an attractive class of strained aromatic compounds of theoretical and synthetic interests In the literature it has been scaresely come accross with the above mentioned parent tricyclo compounds and/or their BN-bond(s) embedded derivatives [10]. However, in some they have been the points of interest indirect way [10-14]. However, general access to these compounds, especially those that are functionalized, is quite limited [10].

2. Method of Calculations

In the present study, all the initial optimizations of the structures leading to energy minima have been achieved first by using MM2 method which is then followed by semi empirical PM3 self consistent fields molecular orbital method [15-17]. Afterwards, the structure optimizations have been achieved within the framework of Hartree-Fock and finally by using density functional theory (DFT) at the level of B3LYP/6-311++G(d,p) [18,19]. Note that the exchange term of B3LYP consists of hybrid Hartree-Fock and local spin density (LSD) exchange functions with Becke's gradient correlation to LSD exchange [20]. The correlation term of B3LYP consists of the Vosko, Wilk, Nusair (VWN3) local correlation functional [21] and Lee, Yang, Parr (LYP) correlation correction functional [22]. In the present study, the normal mode analysis for each structure yielded no imaginary frequencies for the $3N–6$ vibrational degrees of freedom, where N is the number of atoms in the system. This search has indicated that the structure of each molecule considered corresponds to at least a local minimum on the potential energy surface. Furthermore, all the bond lengths have been thoroughly searched in order to find out whether any bond cleavages occurred or not during the geometry optimization process. All these computations were performed by using SPARTAN 06 program [23].

3. Results and Discussion

Optimized structures as well as the direction of the dipole moment vectors of the parent isomers, A and B considered, are shown in Figure 2. They are planar molecules.

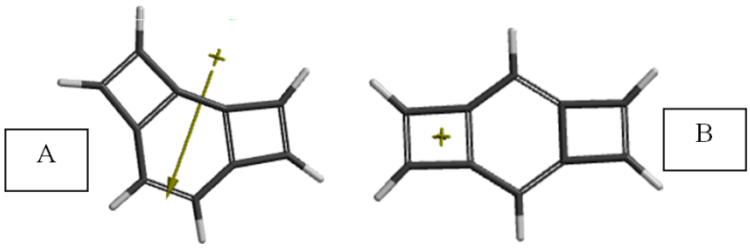

Figure 1. Optimized structures of parent molecules considered.

Similarly, Figures 2 and 3 stand for A and B series of BN bond possessing (constituted by trivalent boron and nitrogen atoms) isomeric structures which include the regioisomers. Of them, A3 and B2 are decomposed

ones having elongated B-N bonds/distances (2.77 and 2.78 Å, respectively). All A- and B-series of structures are planar too. Note that even, highly distorted structures A3 and B2, are coplanar. Note the variation of direction of dipole moment vectors in the regioisomers.

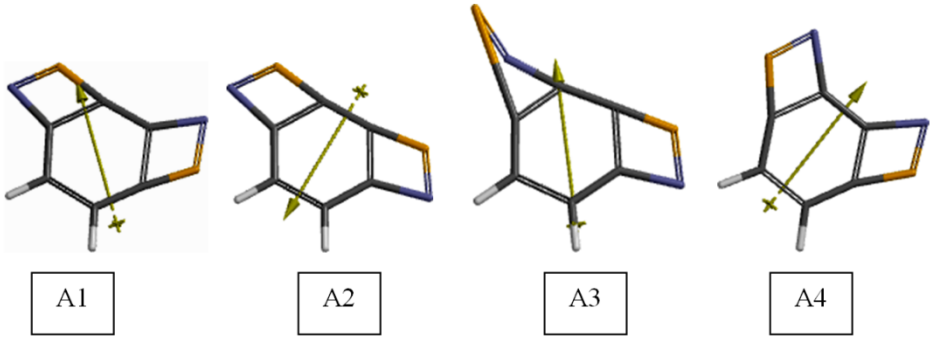

Figure 2. Optimized A-series of structures.

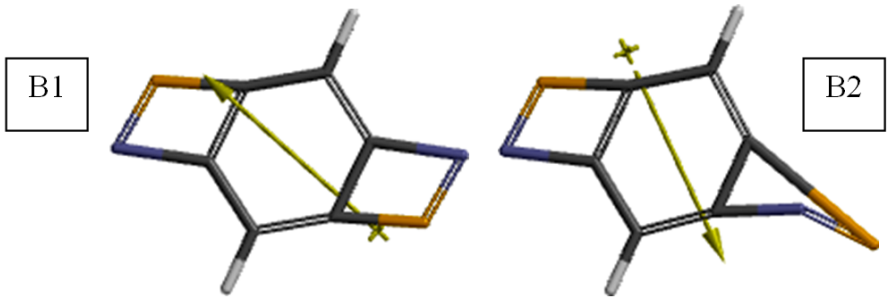

Figure 3. Optimized B-series of structures.

Table 1 contains some thermo chemical properties of the species considered. Whereas, Table 2 includes some energies of them. The data in Table 1 reveal that the standard heat of formation (Hº) values of the species are exothermic and they are favored according to their Gº (Gibbs free energy of formation) values. Isomer-A is more exothermic and more stable than isomer-B. The algebraic order of Hº and Gº values in series-A is A1<A2<A4<A3. Whereas in series-B the order is B1<B2. The variations of these values among each set of structures seem to be related to bond angles and bond lengths of the rings present (see Figures 4-6).

Table 1. Some thermo chemical properties of the species considered.

Structures	Hº	Sº (J/molº)	Gº
A	-1009395.539	344.27	-1009498.184
A1	-1020888.478	346.23	-1020991.708
A2	-1020847.974	344.95	-1020950.821
A3	-1020612.228	355.65	-1020718.268
A4	-1020836.361	347.31	-1020939.912
B	-1009327.221	347.22	-1009430.745
B1	-1020839.827	346.18	-1020943.044
B2	-1020612.848	355.96	-1020718.979

Energies in kJ/mol.

Note that in Table 2, E, ZPE and E_C stand for the total electronic energy, zero point vibrational energy and the corrected total electronic energy, respectively [23]. The data in Table 2 reveal that they are all electronically favorable structures at the standard states.

Table 2. Some energies of the species considered.

Structures	E	ZPE	E_C
A	-1009721.45	314.65	-1009406.8
A1	-1021079.61	179.51	-1020900.12
A2	-1021039.66	180.12	-1020859.54
A3	-1020799.81	175.02	-1020624.79
A4	-1021028.02	180.03	-1020847.99
B	-1009650.44	311.50	-1009338.94
B1	-1021031.34	179.84	-1020851.58
B2	-1020799.49	174.07	-1020625.42

Energies in kJ/mol.

The calculated bond lengths/distances of the species considered are shown in Figures 4-6. In Figures 4-6 the bond lengths of the rings show some kind of alternance of long and short type.

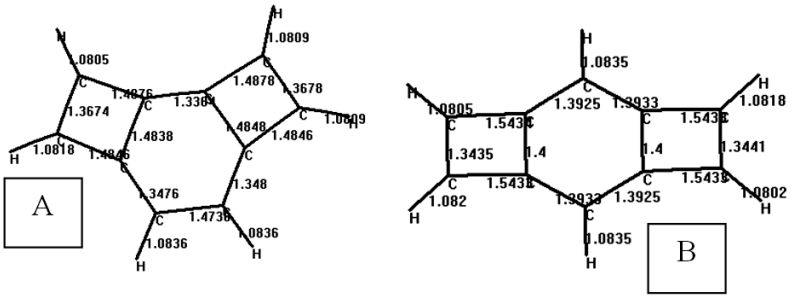

Figure 4. Calculated bond lengths of the parent molecules.

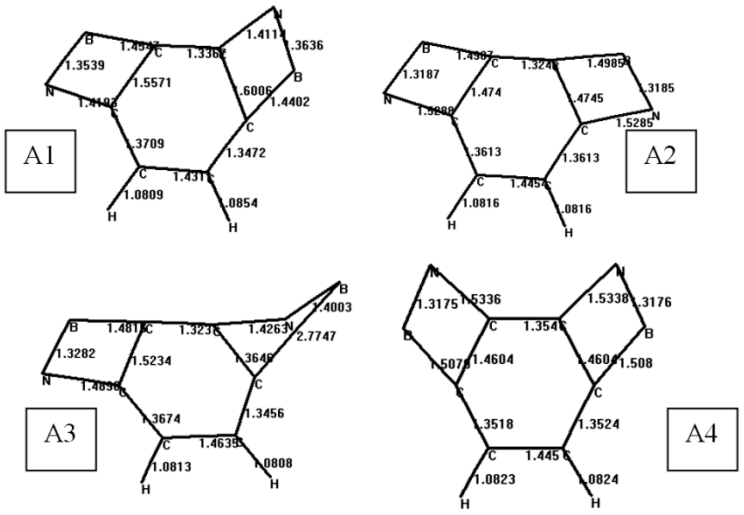

Figure 5. Calculated bond lengths/distances of A-series structures.

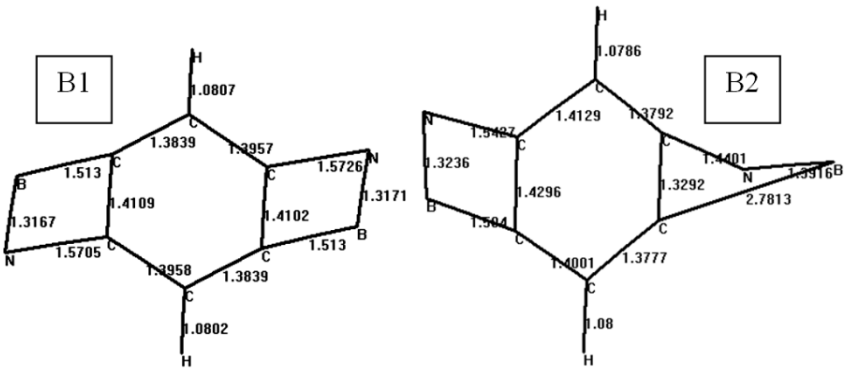

Figure 6. Calculated bond lengths/distances of B-series structures.

Figures 7-9 display the electrostatic potential (ESP) maps of the species considered where negative potential regions reside on red/reddish and positive ones on blue/bluish parts of the maps. The ESP charge distributions in 4-membered rings of the parent structures are such that they are positive at the fusion points but negative at the other peripheral carbon atoms. So some electron population shift occurs from phenylene ring to the 4-membered rings.

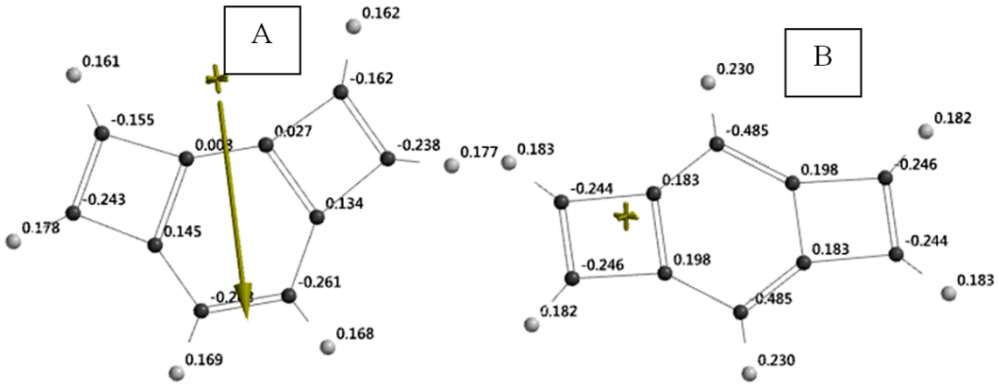

Figure 7. The ESP charges on atoms of the parent compounds considered.

As for the perturbed structures, the charge distribution exhibits that the boron atoms are all positive, whereas adjacent nitrogens are negative, except structure-3. Since in the parent hydrocarbons considered, those positions (subjected to perturbations) are negatively charged, the emergence of negatively charged boron atoms after perturbation should arise if borons take the role of acting as sinks (which disappears in A3 case) for electrons. As the distortion occurs the boron and nitrogen atoms exchange their roles.

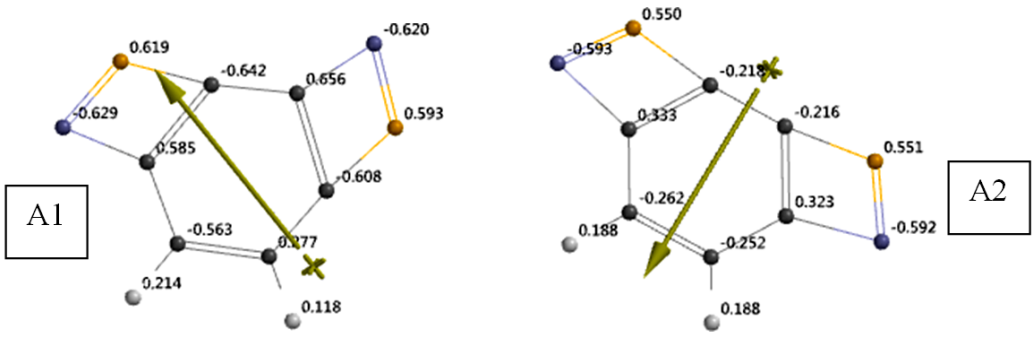

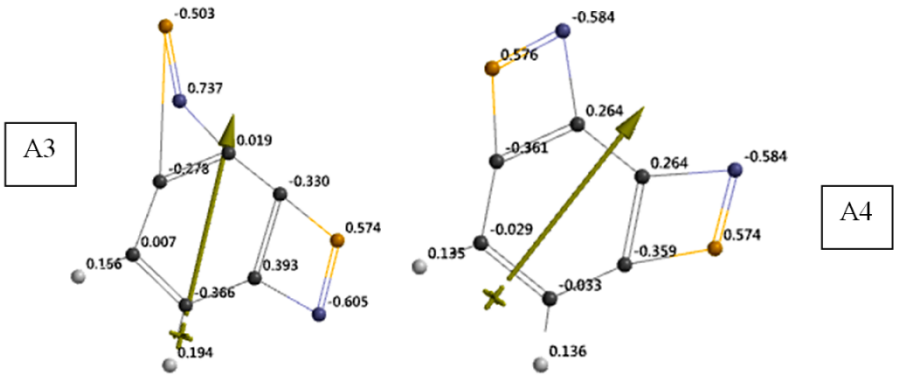

Figure 8. The ESP charges on atoms of A-series of compounds considered.

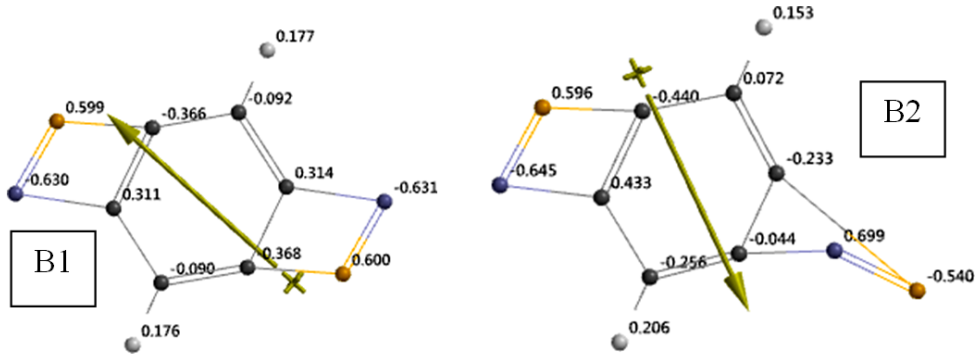

Figure 9. The ESP charges on atoms of B-series of compounds considered.

Table 3 lists some properties of the species considered. The polarizability is defined according to a multivariable formula which is a function of Van der Waals volume and hardness [23]. The later one is dictated by molecular orbital energies of the highest occupied (HOMO) and the lowest unoccupied (LUMO) molecular orbital energies (see the following sections).

Table 3 reveals that the BN-perturbation presently considered lowers Cv values in all the cases. The dipole moments and polarizabilities are deprived of any generalization and highly structure dependent.

Table 3. Some properties of the species considered.

Structures	Dipole (debye)	Polarizability	Cv (J/mol^o)
A	0.47	52.42	103.52
B	0.00	52.68	105.04
A1	2.80	51.27	97.56
A2	2.18	51.52	98.40
A3	1.35	52.05	98.82
A4	6.30	51.41	98.41
B1	0.01	51.50	96.56
B2	3.74	52.13	97.46

Structures A and B posses formula of $C_{10}H_6$, the other structures have $C_6H_2B_2N_2$. The aqueous energies of A and B are -1009739.50 and -1009666.63 kJ/mol., respectively.

Figures 10-12 show electrostatic potential maps of the structures presently considered. In the perturbed structures depending on the regioisomerism, sometimes borons sometimes the adjacent nitrogen atoms appear in positive or negative potential regions.

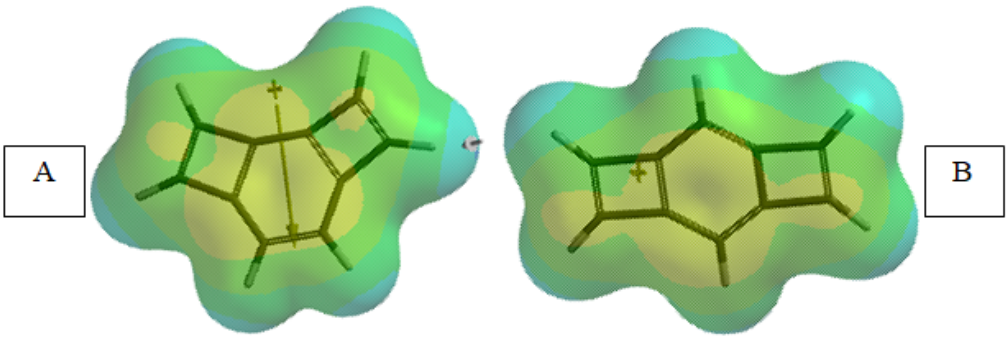

Figure 10. Electrostatic potential maps of the parent structures.

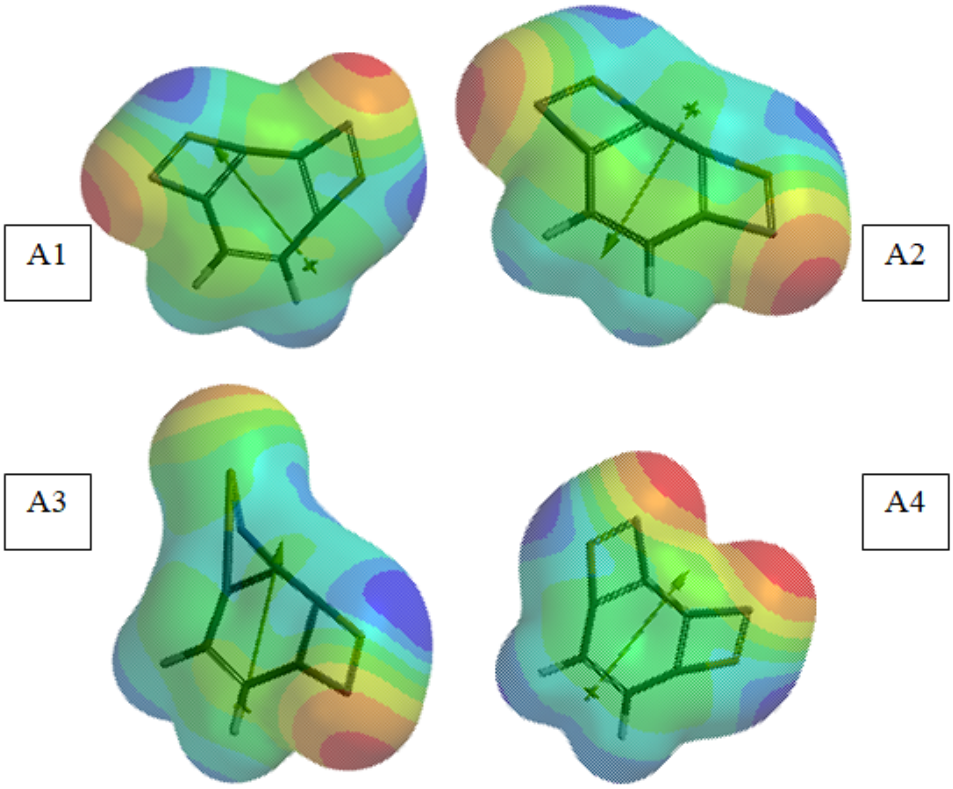

Figure 11. Electrostatic potential maps of A-series of structures.

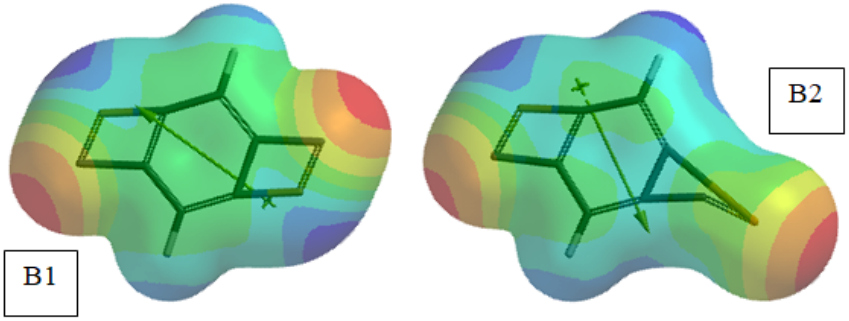

Figure 12. Electrostatic potential maps of B-series of structures.

Figures 13-15 show the local ionization maps of the species considered where conventionally red/reddish regions (if any exists) on the density surface indicate areas from which electron removal is relatively easy, meaning that they are subject to electrophilic attack. Note that the local ionization potential map is a graph of the value of the local ionization potential on an isodensity surface corresponding to a van der Waals surface.

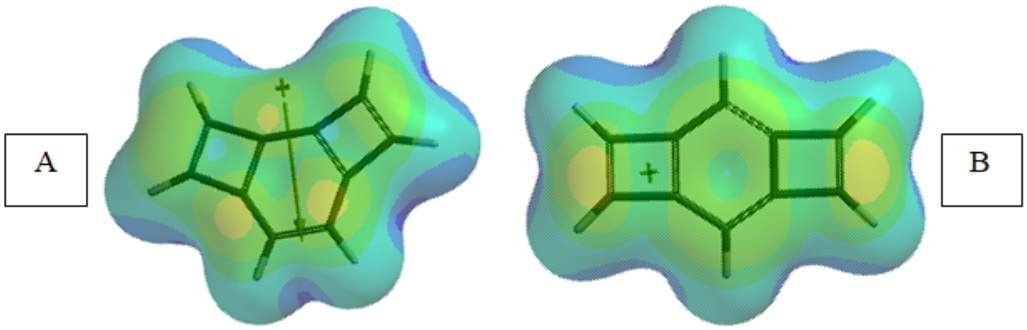

Figure 13. Local ionization potential maps of the parent structures.

Among the local ionization potential maps shown in Figure 14, the map of A3 (similarly B2) is striking. The distortion/ rupture highly perturbs the potential field compared to the others.

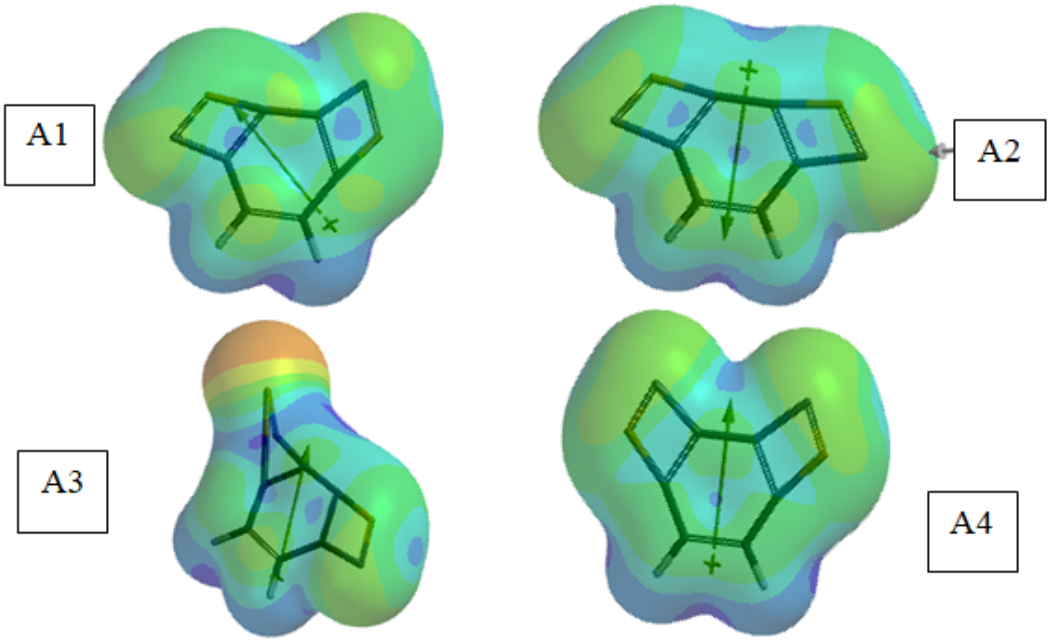

Figure 14. Local ionization potential maps of A-series of structures

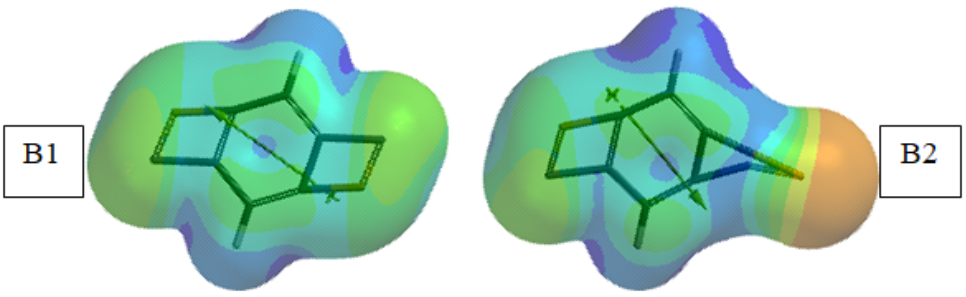

Figure 15. Local ionization potential maps of B-series of structures.

The LUMO maps of the species presently considered are shown in Figures 16-18. Note that a LUMO map displays the absolute value of the LUMO on the electron density surface. The blue color (if any exists) stands for the maximum value of the LUMO and the red colored region, associates with the minimum value. It is to be noted that the LUMO and NEXTLUMO (LUMO+1) are the major orbitals directing the molecule towards the attack of nucleophiles [23]. Positions where the greatest LUMO coefficient exists is the most vulnerable site in nucleophilic reactions. As seen in the LUMO maps BN bond highly change absolute value of the LUMO on the electron density surface.

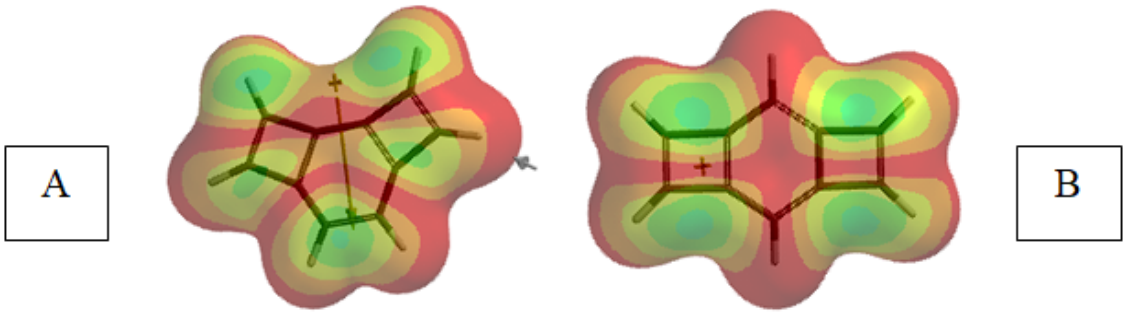

Figure 16. The LUMO maps of the parent structures.

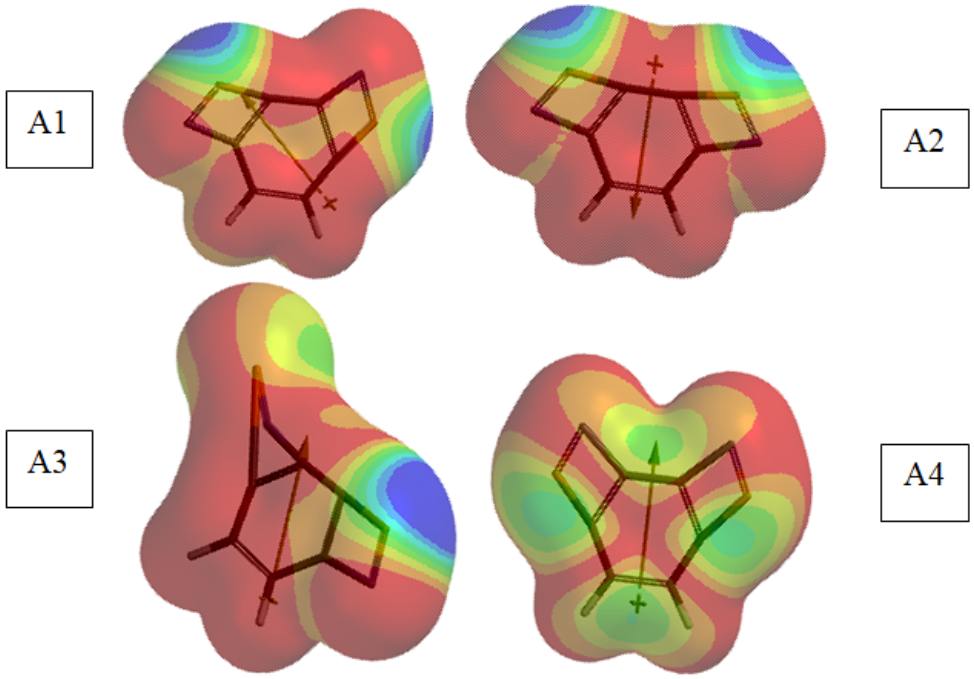

Figure 17. The LUMO maps of A-series of structures.

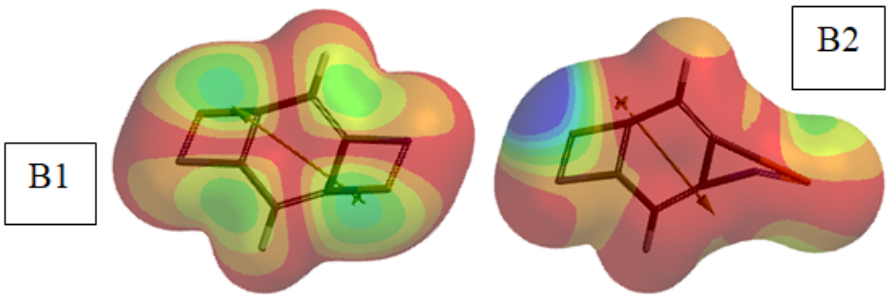

Figure 18. The LUMO maps of B-series of structures.

Figures 19-21 show the bond densities of the species considered. The bond density contains fewer electrons in total and demarks atomic connectivity. In the case of parent structures the bond density at the peripheral double bonds of 4-membered rings are noticeable.

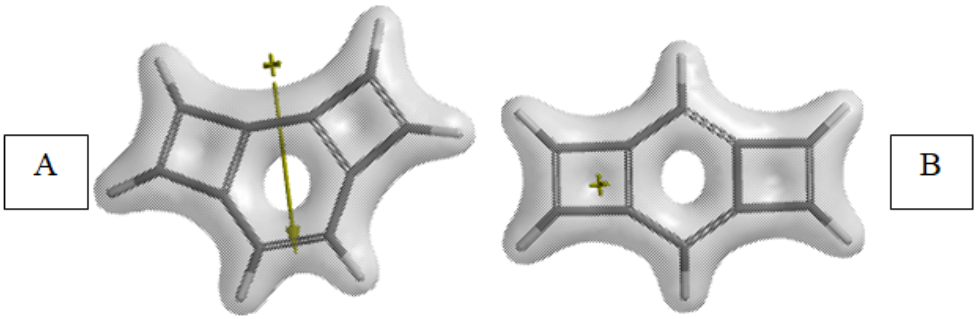

Figure 19. Bond densities of the parent structures.

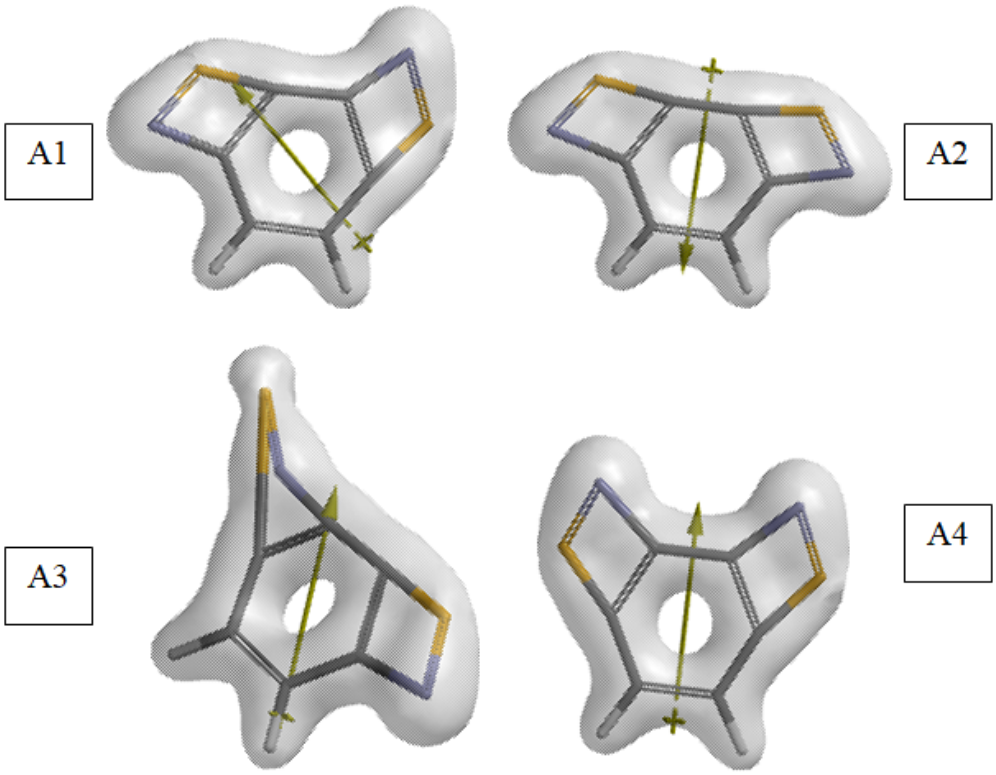

Figure 20. Bond densities of A-series of structures.

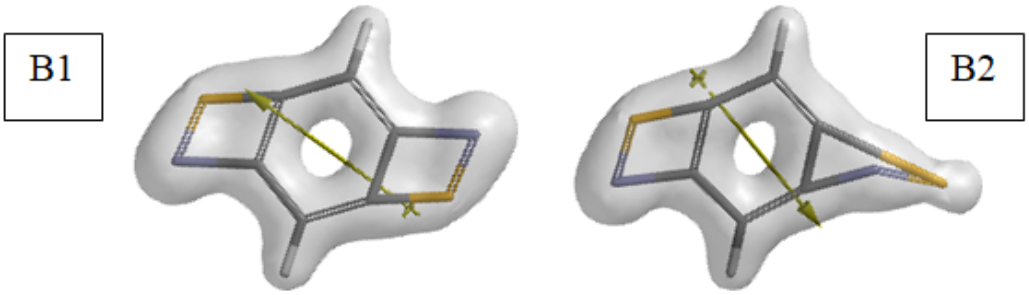

Figure 21. Bond densities of B-series of structures.

As seen in the figures the bond density around the nitrogen atoms, (also about the BN bonds) is quite high. All these arise from the elrctronegativities and donor/ acceptor properties of the nitrogen and boron atoms in those particular structures.

Some of the molecular orbital energy levels of the isomers considered are displayed in Figures 22-24. Note that that the inner lying occupied molecular orbitals are assumed to be responsible for the thermal stability of the compound.

In principle, the parent hydrocarbons A and B are even alternant hydrocarbons [5]. Their molecular orbital energy levels should be oriented symmetrically about the zero energy level. In the present DFT level and the considered basis set some properties of even alternant hydrocarbons have been modified. That perturbation is even more drastic when BN bond insertion occurs. The bond lengths and bond angles vary even from regioisomer to regio isomer. It is true not only for the 4-membered rings but also for the phenylene nucleus of the isomers considered, which reminds Mills- Nixon Effect [24,25].

As seen in Figure 22 structural variations between the parent hydrocarbons are accompanied by various lowering or raisings of the molecular orbital energy levels. Those changes not only compromised the frontier molecular orbitals but also the NEXTHOMO and NEXTLUMO levels and some inner lying occupied levels (see Table 4).

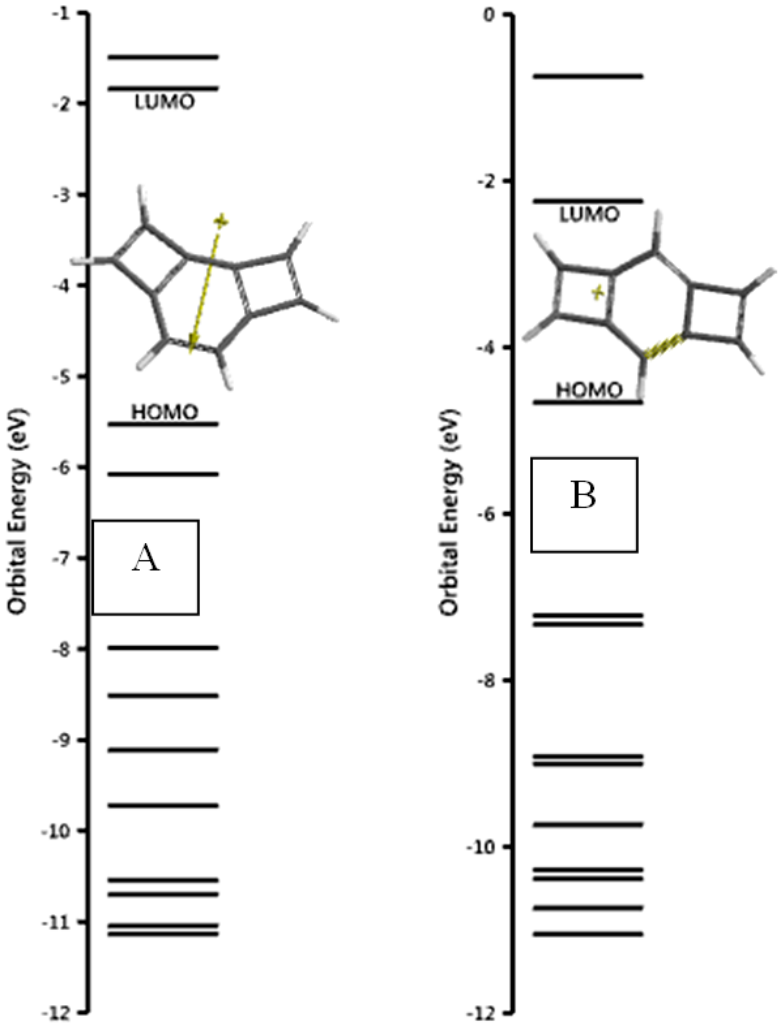

Figure 22. Some of the orbital energies of the parent compounds considered.

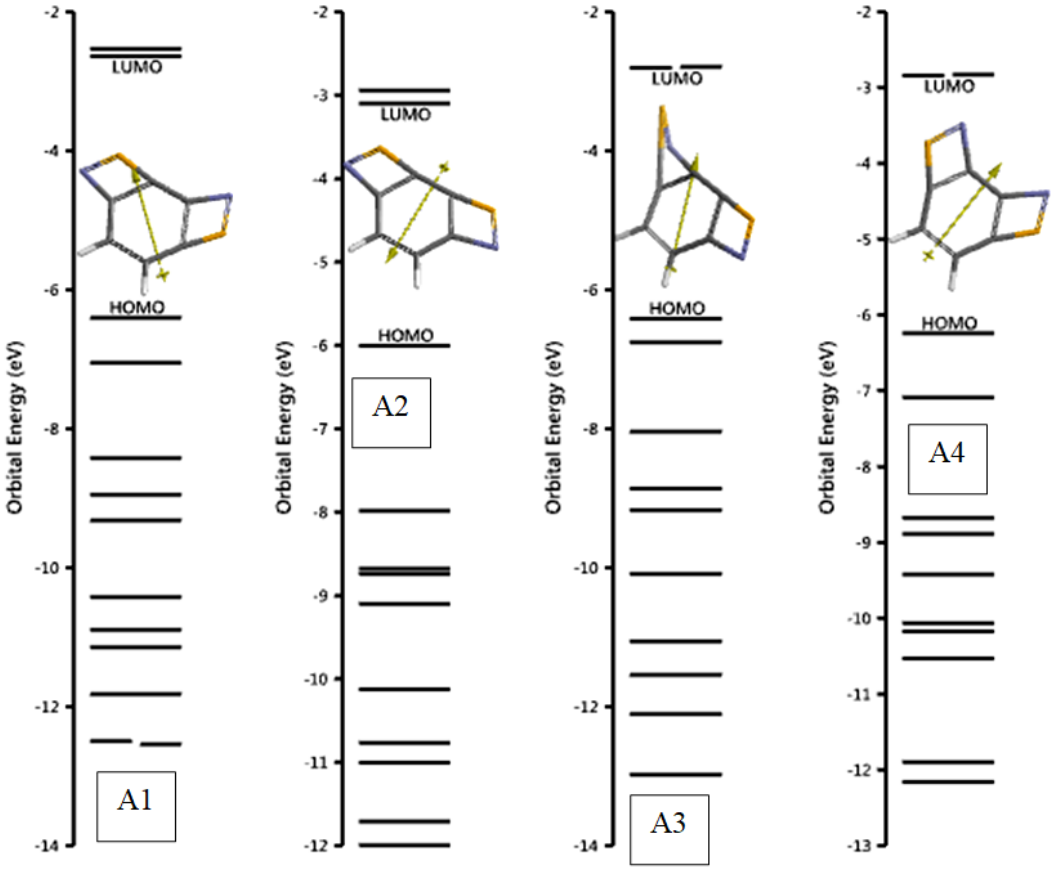

Figure 23. Some of the orbital energies of A-series of compounds of interest.

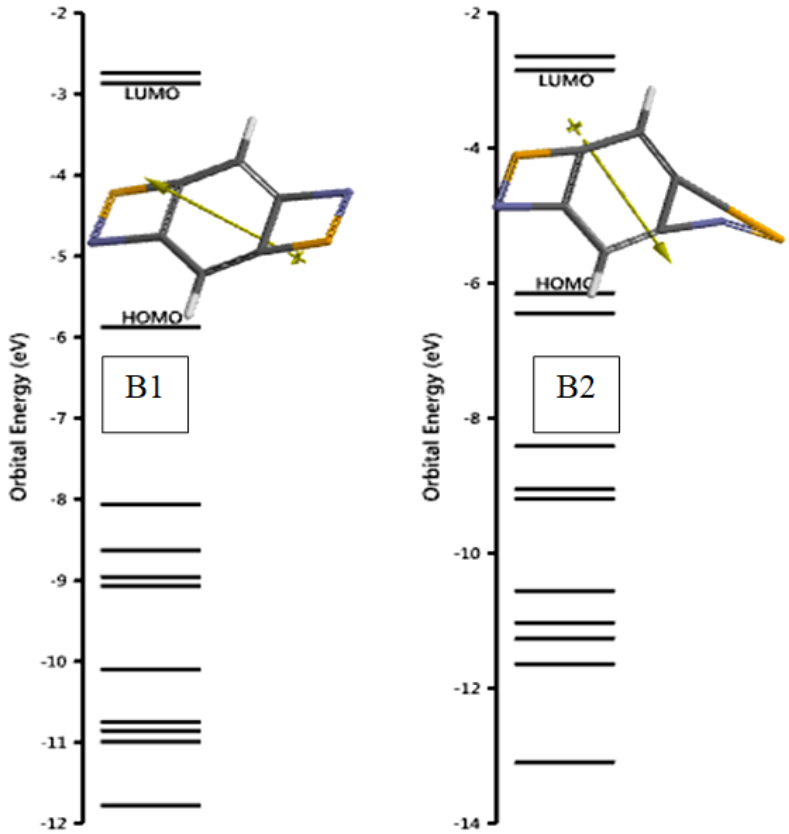

Figure 24. Some of the orbital energies of B-series of compounds of interest.

The HOMO and LUMO energies and interfrontier molecular orbital energy gap values, Δε (Δε = ε_{LUMO}-ε_{HOMO}) of the isomers considered are included in Table 4. In general, the BN bond perturbation lowers the HOMO and LUMO energy levels of the parent structures A and B, acting as an electron deficient substituent.

Table 4. The HOMO and LUMO energies and Δε values of the species considered.

Structures	HOMO	LUMO	Δε
A	-533.32	-177.05	356.27
A1	-617.62	-254.38	363.24
A2	-579.37	-299.32	280.05
A3	-619.06	-270.42	348.64
A4	-602.24	-273.82	328.42
B	-449.44	-216.62	232.82
B1	-567.35	-276.55	290.80
B2	-593.79	-274.59	319.20

Energies in kJ/mol.

Time dependent density functional UV-VIS spectra of the isomers of interest are shown in Figure 25. The spectra of the parent hydrocarbons (they are isomers) are very different because structure-B has more elongated conjugated path for π-electrons (extended conjugation [5,26]) whereas possibilities of the extended conjugation and Clar's sextet [27,28] in structure-B are two factors principally opposing to each other. So some of the bonds tends to be essentially single/double [5]. The other spectra exhibit variations depending on the particular effects on the spectrums thus variations due to the regioisomers are to be obtained and indeed they are the case Note the spectra of A, A2; A2, A3; A3, A4 and also B1, B2. As seen in the figure, in some A-series of isomer bathochromic effect [31] arises parallel to the extended conjugation. Whereas some of the isomers exhibit hypsochromic effect [31] such as B2 as compared to its isomer, B1. Not only the λ_{max} values but also the intensities of the peaks are function of many factors. One of them is related to magnitudes of the transition moments between the orbitals involved in the transition which vary from isomer to isomer [29,30].

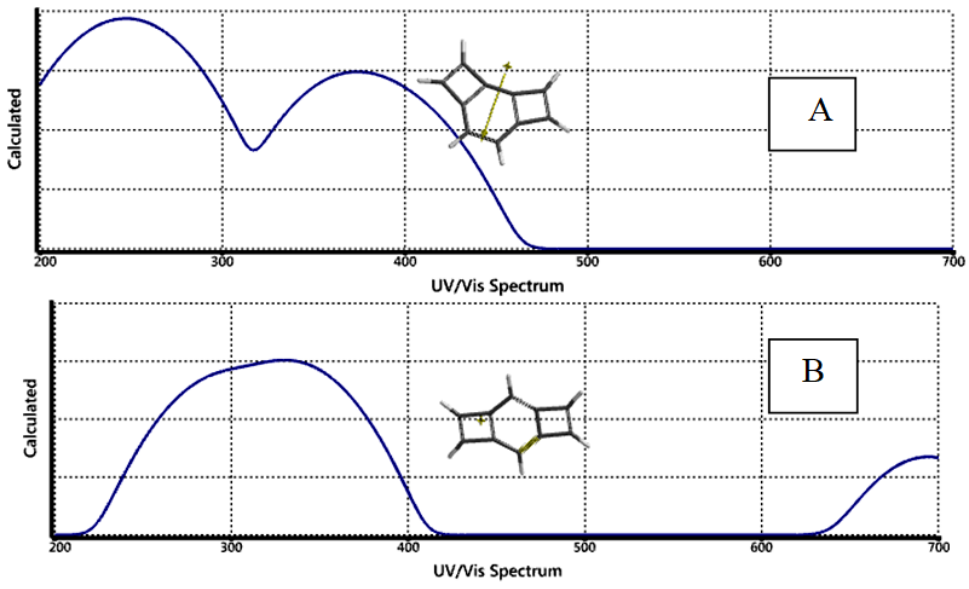

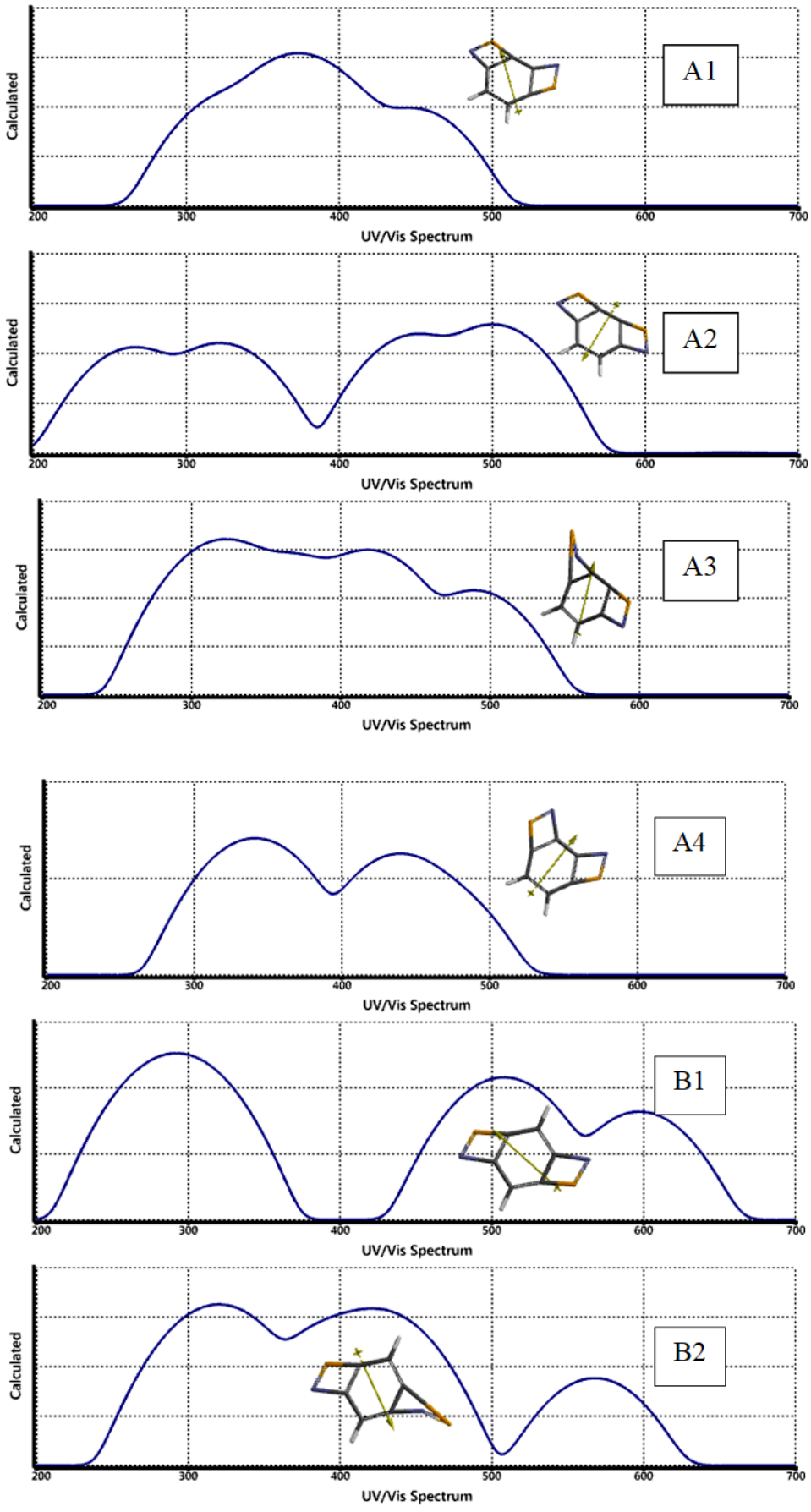

Figure 25. Time dependent density functional UV-VIS spectra of the species of interest.

4. Conclusion

Perturbation effects of two BN-bonds on two tricyclo pentaene structures consisting of 10-ring atoms in their π-skeleton and two cyclobutene rings annealed have been considered. The parent structures and their perturbed forms have been found to be thermally favored and electronically stable at the standard states. In all the cases, the bond lengths of the rings show some kind of alternance of long and short type. The ESP charge distributions in 4-membered rings of the parent structures are such that they are positive at the fusion points but negative at the other peripheral carbon atoms. So some electron population shift occurs from phenylene ring to the 4-membered rings. The charge distribution in the perturbed structures exhibits that in general, the boron atoms are all positive, whereas adjacent nitrogens are negative. The elrctronegativities and donor/ acceptor properties of the nitrogen and boron atoms in those particular structures dictate the bond densities in such a way that the bond densities around the nitrogen atoms, also about the BN bonds are quite high. . In general, the BN bond perturbation lowers the HOMO and LUMO energy levels of the parent structures A and B, acting as an electron deficient substituent. The time dependent UV-VIS spectra show variations depending on the regioisomer structure and some exhibit bathochromic effect some hypsochromic effect within the series of isomer considered.

References

[1] Huang, J., & Li, Y. (2018). BN embedded polycyclic π-conjugated systems: Synthesis, optoelectronic properties, and photovoltaic applications. *Frontiers in Chemistry*, *6*, 341. https://doi.org/10.3389/fchem.2018.00341

[2] Butenschön, H. (2007). A new oxocarbon $C_{12}O_6$ via highly strained benzyne intermediates. *Angewandte Chemie*, *46*(22), 4012–4014. https://doi.org/10.1002/anie.200700926

[3] Hamura, T., Ibusuki, Y., Uekusa, H., Matsumoto, T., & Suzuki, K. (2006). Poly-oxygenated tricyclobutabenzenes via repeated [2 + 2] cycloaddition of benzyne and ketene silyl acetal. *Journal of the American Chemical Society*, *128*, 3534–3535. https://doi.org/10.1021/ja0602647

[4] Zachary, X.G., & Shih-Yuan, L. (2018). The state of the art in azaborine chemistry: New synthetic methods and applications. *Journal of the American Chemical Society*, *140*(4), 1184–1194. https://doi.org/10.1021/jacs.7b09446

[5] Dewar, M.J.S., & Dougherty, R.C. (1975). *The PMO theory of organic chemistry*. New York: Plenum/Rosseta.

[6] Edel, K., Yang, X., Ishibashi, J.S.A., Lamm, A.N., Maichle-Mössmer, C., Giustra, Z.X., Liu, S.Y., & Bettinger, H.F. (2018). The Dewar isomer of 1,2-dihydro-1,2-azaborinines: isolation, fragmentation, and energy storage. *Angewandte Chemie International Edition*, *57*(19), 5296–5300. https://doi.org/10.1002/anie.201712683

[7] Burford, R.J., Li, B., Vasiliu, M., Dixon, D.A., & Liu, S.Y. (2015). Diels–Alder reactions of 1,2-azaborines. *Angewandte Chemie International Edition*, *54*(27), 7823–7827. https://doi.org/10.1002/anie.201503483

[8] Campbell, P.G., Marwitz, A.J., & Liu, S.Y. (2012). Recent advances in azaborine chemistry. *Angewandte Chemie International Edition*, *51*(25), 6074–6092. https://doi.org/10.1002/anie.201200063

[9] Giustra, Z.X., & Liu, S.Y. (2018). The state of the art in azaborine chemistry: New synthetic methods and applications. *Journal of the American Chemical Society*, *140*(4), 1184–1194. https://doi.org/10.1021/jacs.7b09446

[10] Arisawa, T., Hamura, T., Uekusa, H., Matsumoto, T., & Suzuki, K. (2008). Linearly fused dicyclobutabenzenes via dual, regioselective cycloadditions of 1,4-benzdiyne equivalent and ketene silyl acetals: Synthesis of linearly fused dicyclobutabenzenes. *Synlett*, *8,* 1179–1184. https://doi.org/10.1055/s-2008-1072729

[11] Toda, F., & Mukai, K. (1975). An evidence for singlet ground state of 1,6-di-*t*-butyl-3,4,8,9-tetraphenyltricyclo[6.2.0.$0^{2,5}$]deca-1,3,5,7,9-pentaene, *Chemistry Letters*, *4*(7), 777–778. https://doi.org/10.1246/cl.1975.777

[12] Roth, W.R., Langer, R., Ebbrecht, T., Beitat, A., & Lennartz, H.-W. (1991). Zur Energie Delle von Diradikalen; III. 2,3,5,6-Tetramethylen-1,4-cyclohexadiyl. *Chemische Berichte*, *124*(12), 2751–2760.

[13] Siegel, J.S. (1994). Mills–Nixon effect: Wherefore art thou? *Angewandte Chemie International Edition*, *33*, 1721–1723. https://doi.org/10.1002/anie.199417211

[14] Frank, N.L., & Siegel, J.S. (1995). Advances in theoretically interesting molecules. In R.P. Thummel (Ed.), *Advances in theoretically interesting molecules* (Vol. 3, pp. 209–260). Greenwich, USA: JAI Press.

[15] Stewart, J.J.P. (1989). Optimization of parameters for semi-empirical methods I. *Journal of Computational Chemistry*, *10*, 209–220. https://doi.org/10.1002/jcc.540100208

[16] Stewart, J.J.P. (1989). Optimization of parameters for semi-empirical methods II. *Journal of Computational Chemistry, 10*, 221–264. https://doi.org/10.1002/jcc.540100209

[17] Leach, A.R. (1997). *Molecular modeling*. Essex: Longman.

[18] Kohn, W., & Sham, L.J. (1965). Self-consistent equations including exchange and correlation effects. *Physical Review*, *140*, 1133–1138. https://doi.org/10.1103/PhysRev.140.A1133

[19] Parr, R.G., & Yang, W. (1989). *Density functional theory of atoms and molecules*. London: Oxford University Press.

[20] Becke, A.D. (1988). Density-functional exchange-energy approximation with correct asymptotic behavior. *Physical Review A*, *38*, 3098–3100. https://doi.org/10.1103/PhysRevA.38.3098

[21] Vosko, S.H., Wilk, L., & Nusair, M. (1980). Accurate spin-dependent electron liquid correlation energies for local spin density calculations: a critical analysis. *Canadian Journal of Physics, 58*, 1200–1211. https://doi.org/10.1139/p80-159

[22] Lee, C., Yang, W., & Parr, R.G. (1988). Development of the Colle-Salvetti correlation energy formula into a functional of the electron density. *Physical Review B*, *37*, 785–789. https://doi.org/10.1103/PhysRevB.37.785

[23] Wavefunction Inc. (2006). *SPARTAN 06*. Irvine, CA, USA.

[24] Maksić, Z.B., & Orville-Thomas, W.J. (Eds.). (1999). *Pauling's legacy: Modern modelling of the chemical bond*. Theoretical and Computational Chemistry (Vol. 6). Amsterdam, The Netherlands: Elsevier.

[25] Stanger, A. (1991). Is the Mills-Nixon effect real? *Journal of the American Chemical Society*, *113*(22), 8277–8280. https://doi.org/10.1021/ja00022a012

[26] Fleming, I. (1976). *Frontier orbitals and organic reactions*. London: Wiley.

[27] Clar, E. (1972). *The aromatic sextet*. London: Wiley.

[28] Clar, E. (1964). *Polycyclic hydrocarbons* (Vol. 1). London: Academic Press.

[29] Anslyn, E.V., & Dougherty, D.A. (2006). *Modern physical organic chemistry*. Sausalito, California: University Science Books.

[30] Turro, N.J. (1991). *Modern molecular photochemistry.* Sausalito: University Science Books.

[31] Ferguson, L.N. (1969). The modern structural theory of organic chemistry, New Delhi: Prentice-Hall of India.